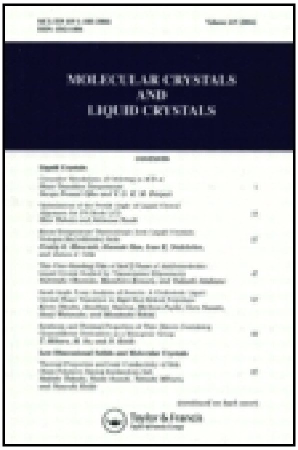

Molecular Crystals and Liquid Crystals
Publication details, including instructions for authors and subscription information:
http://www.tandfonline.com/loi/gmcl20

Amplification of Laser Emission from Cholesteric Liquid Crystals by Planar Cells with Laser Dye Nematic and Isotropic Solutions

N. M. Shtykov [a] , M. I. Barnik [a] , V. V. Lazarev [a] , S. P. Palto [a] , B. A. Umanskii [a] , L. M. Blinov [a] [b] & G. Cipparrone [b]

[a] Institute of Crystallography, Russian Academy of Science, Moscow, Russia

[b] Lab. Regionale CNR-INFM LICRYL, Physics Department, Calabria University, Rende (CS), Italy

Version of record first published: 05 Apr 2011

To cite this article: N. M. Shtykov, M. I. Barnik, V. V. Lazarev, S. P. Palto, B. A. Umanskii, L. M. Blinov & G. Cipparrone (2008): Amplification of Laser Emission from Cholesteric Liquid Crystals by Planar Cells with Laser Dye Nematic and Isotropic Solutions, Molecular Crystals and Liquid Crystals, 494:1, 258-271

To link to this article: http://dx.doi.org/10.1080/15421400802429929

Mol. Cryst. Liq. Cryst., Vol. 494, pp. 258–271, 2008
Copyright © Taylor & Francis Group, LLC
ISSN: 1542-1406 print/1563-5287 online
DOI: 10.1080/15421400802429929

Amplification of Laser Emission from Cholesteric Liquid Crystals by Planar Cells with Laser Dye Nematic and Isotropic Solutions

N. M. Shtykov[1], M. I. Barnik[1], V. V. Lazarev[1], S. P. Palto[1], B. A. Umanskii[1], L. M. Blinov[1,2], and G. Cipparrone[2]
[1]Institute of Crystallography, Russian Academy of Science, Moscow, Russia
[2]Lab. Regionale CNR-INFM LICRYL, Physics Department, Calabria University, Rende (CS), Italy

A possibility have been shown for amplification of weak emission intensity of microlasers based on cholesteric liquid crystals (CLC) by thin planar layers of both isotropic dye solutions and dye doped nematic liquid crystals. Very high gain index values (up to 500 cm^{-1}) and absolute amplification of about 15 have been demonstrated. Especially important is the anisotropy of gain in nematics, which allows the field control of the light amplification by an electric field. The planar amplifiers using nematic liquid crystals can easily be integrated within single planar devices together with distributed feedback CLC microlasers. In such a hybrid structure, 6-times amplification of CLC microlaser intensity has been achieved.

Keywords: dye lasers; laser amplifiers; liquid crystals

1. INTRODUCTION

Cholesteric liquid crystals (CLC) are helical structures with periodic modulation of the refractive index along the helical axis. They may be considered as one-dimensional photonic crystals [1,2] with a stop-band for light of a certain circular polarization. The spectral

The authors thank Mr. S. V. Yakovlev (ICRAN) and Mr. A. Pane (LiCryL-CNR) for the help in experiment and Prof. E. A. Luk'yanets and Dr. V. I. Alekseeva for supplying the samples of dye Chromene-3. The Russian group was supported by OFN RAN (program "Laser systems based on novel active materials"). The Italian group acknowledges the support from CNR-INFM and the CEMIF.CAL funds.

Address correspondence to L. M. Blinov, Institute of Crystallography, Russian Academy Science, Leninsky pr. 59, Moscow, Russia. E-mail: blinov@fis.unical.it

position of the band is determined by the pitch of the helix P_0 and principal refraction indices of the material, $n_{\perp}P_0 \leq \lambda \leq n_{||}P_0$. Dye-doped CLC are known as materials for compact, low threshold, distributed feedback (DFB) lasers [3,4] emitting narrow band light virtually at any pre-selected wavelength within the whole visible range [5]. The lasing in CLC is usually observed at one of the edges of the stop-band where the maximum density of photon field states is realized [4]. The latter provides the most profound feedback necessary for generation [6].

Thin film CLC microlasers are unique devices because they may be considered as elements (pixels) of a planar matrix structure, similar to the display structure controlled by an electric filed. Indeed, based on pure thermodynamic arguments, de Gennes has predicted a smooth field-induced unwinding of the helical structure (i.e., the stop band position) [7]. However, in reality, one meets principal difficulties not only with a smooth unwinding of the ideal helix by the electric field but also with a step-like unwinding observed, for example, upon a temperature change [8]. These difficulties originate from the topological confinements imposed on the helix unwinding [9], particularly in the external electric field [10].

For this reason, we suggest to entrust the field control function over light emission intensity and polarization from the planar CLC oscillator to a light amplifier based on a nematic liquid crystal (NLC). The CLC oscillator possesses selectivity and is able to generate a narrow spectral band with a small angular divergence. In this case, the signal must be strong enough to overcome broad band optical noise of the amplifier. In turn, planar layers of NLC manifest a strong field controlled optical anisotropy and a variety of electro-optical phenomena [11]. Such an amplifier can be done without cavity as a traveling wave laser [12–14].

Another important advantage of NLC is their fluidity and, as a consequence, a higher resistance to formation of radiation defects. Due to this, they withstand higher pump fluence than CLC. Unfortunately, in CLC, an increase in size of the pump spot at the same pump fluence results in a leakage of energy in all transverse directions that reduces the output energy in the CLC Bragg mode [15]. In fact, long time stable operation of CLC microlasers is limited by pump energy of the order of 1 μJ and output energy of the order of 100 nJ. Therefore, a weak emission of CLC has to be amplified.

In the present work, at first, we show a possibility for the amplification of the CLC laser emission using a planar, uniformly oriented layer of an NLC doped with a lasing dye. In this case, the CLC oscillator and the NLC amplifier are pumped independently, as two different devices. Then we show a possibility to integrate a CLC laser and an amplifier within a unique planar device. In that case the amplifier is based on the isotropic solution of a laser dye [16] which can, in principle, be substituted by the NLC solution. In both cases, we have obtained a substantial amplification of the output energy of our CLC lasers (15 and 6 times, respectively).

2. CLC OSCILLATOR WITH A SEPARATED NLC AMPLIFIER

The set-up designed in the Institute of Crystallography, Moscow is schematically shown in the Inset to Figure 1. The element G represents a CLC oscillator whose output energy is amplified by the NLC cell A. For both devices a longitudinal pump scheme is used. The beam of a Q-switched Nd^{3+} YAG laser (Model LQ529, Solar; 2nd harmonic, $\lambda = 532$ nm; pulse duration $\tau = 11$ ns; repetition frequency $f = 1$ Hz) propagates from the right side and is divided into two beams by the first beam splitter 1. The transmitted beam is used to pump the amplifier whereas the deviated beam pumps the oscillator. The energy of the two beams can be changed with neutral filters. The lasing spectra of

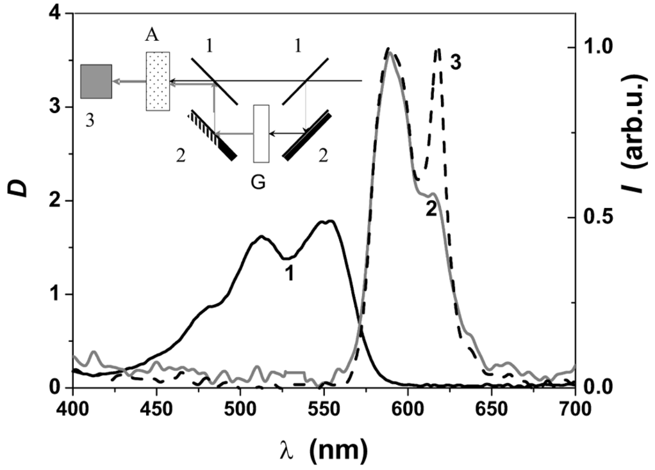

FIGURE 1 Spectra of optical density (D, curve 1) and luminescence of dye Chromene-3 in LJK-2 matrix. Curves 2 and 3 correspond to pump fluence of 7.4 and 11 mJ/cm^2 and normalised to the luminescence intensity at $\lambda = 588$ nm (here, a lens collected luminescence light has been used). Inset: scheme of the setup for measurements of light amplification with oscillator cell G, amplifying cell A, beam splitters 1, mirrors 2, CCD spectrometer 3.

the CLC oscillator before and after amplification were recorded by a CCD spectrometer (S-150-II, resolution of 0.17 nm). The absolute values of the pump and emitted beam energy were measured by a power/energy meter and a calibrated pyroelectric detector, respectively.

The oscillator cell G consisted of two glass plates with a 30 μm gap in between and inner surfaces covered with thin (50 nm) polyimide layers rubbed unidirectionally to provide a good quality planar CLC texture. A home made nematic mixture LJK2 was doped with a chiral compound and 0.3 wt. % of dye Oxazine-17. The resultant mixture had a helical pitch of $P_0 = 383\,\text{nm}$ and principal refraction indices of $n_{\perp} = 1.487$ and $n_{||} = 1.595$ (t = 24°C, $\lambda = 560\,\text{nm}$). The spectral position of the stop band of the mixture ($\lambda = 576$–$615\,\text{nm}$) was completely overlapped by the luminescence spectra of Oxazine-17 ($\lambda = 550$–$650\,\text{nm}$). At the same time, the maximum of the absorption spectrum of the mixture ($\lambda_{\max} = 540\,\text{nm}$) was very close to the pump wavelength. The laser oscillation appears at the long-wavelength edge of the stop band ($\lambda_g = 615.5\,\text{nm}$).

The amplifying cell A is similar to cell G but somewhat thicker, $d = 50\,\mu\text{m}$. The alignment polyimide layers provide a homogeneous planar orientation of the nematic LJK-2 mixture, doped with 0.25 wt. % % laser dye Chromene-3. The absorption and luminescence spectra of the dye doped LJK-2 are shown in Figure 1 for two different values of the pump beam fluence. It is seen that with increasing fluence a narrow band of amplified spontaneous emission (ASE) develops that corresponds to the range of the maximum gain of the dye (~610–620 nm).

A lasing spectrum of the CLC oscillator before amplification (W_0) is shown in Figure 2 (curve 1). Its width (FWHM ≈0.3 nm) is determined by the spectrometer resolution. Curve 2 represents a wider ASE spectrum of the amplifying NLC measured without input signal. The ASE maximum is shifted from the signal spectrum to longer wavelengths only by 2 nm. This provides a strong amplification of the signal, see curve 3. The amplification coefficient at $\lambda_g = 615.5\,\text{nm}$ is $K = W/W_0 \approx 15$ corresponding to amplification index (or negative absorption coefficient)

$$\gamma = 1/d\ \ln K \tag{1}$$

equal to $0.054\,\mu\text{m}^{-1}$ or $540\,\text{cm}^{-1}$. It is very high value that will be discussed later on. With increasing amplitude of the injected signal, the value of amplification decreases 3 times (curve 2 in Fig. 3). The latter is indicative of the saturation regime of the amplifier [17,18]. As expected, the amplification coefficient increases with increasing pump fluence. For example, at the input signal energy of 1.9 nJ, the amplification is growing from $K = 1.2$ at $I_p = 15\,\text{mJ/cm}^2$ up to 4.5 at $41\,\text{mJ/cm}^2$ (curve 1 in Fig. 3).

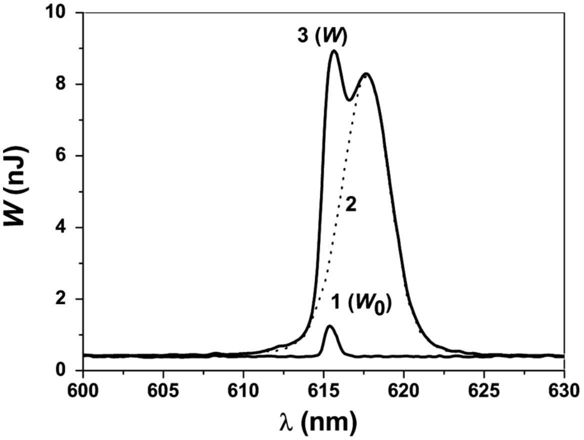

FIGUGRE 2 Emission energy (W) spectrum of lasing cell G at $\lambda = 615.7\,\mathrm{nm}$ measured at the input of the amplifying cell A (curve 1) and emission spectra at the output of amplifier A in the absence (curve 2 and presence (curve 3) of the injected input signal. Pump fluence $I_p = 41\,\mathrm{mJ/cm^2}$.

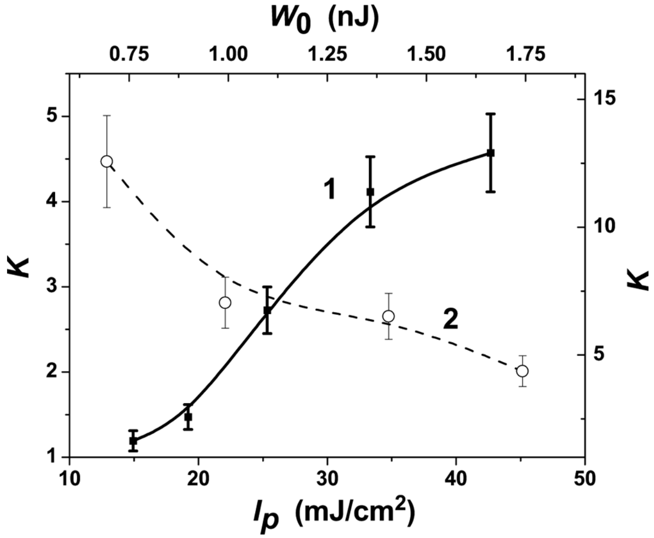

FIGURE 3 Amplification coefficient K vs pump fluence (curve 1, bottom and left scales) at a fixed input signal energy $W_0 = 1.9\,\mathrm{nJ/pulse}$ and the same coefficient K vs input signal energy (curve 2, top and right scales) at a fixed pump fluence $I_p = 41\,\mathrm{mJ/cm^2}$.

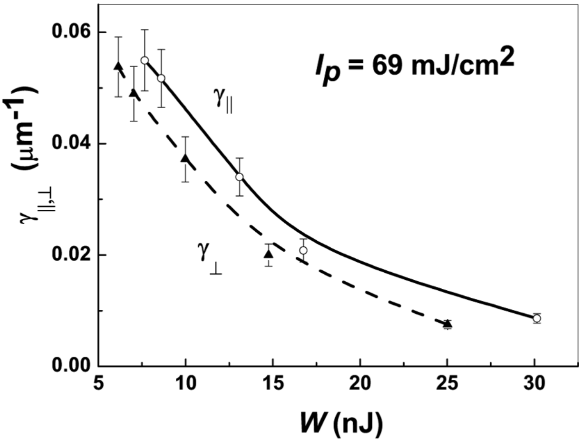

FIGURE 4 Principal gain indices as functions of the amplified pulse energy *W*.

A strong anisotropy of NLC properties manifests itself in the amplification effect. The results of the measurements of gain index γ for two orthogonal linear polarizations, parallel and perpendicular to the NLC director are shown in Figure 4. It is seen that the gain anisotropy is positive, $\gamma_{||} > \gamma_{\perp}$. In particular, the gain indices at a small signal and the pump fluence of 69 mJ/cm^2 are $\gamma_{||} = 0.066\,\mu\text{m}^{-1}$ and $\gamma_{\perp} = 0.056\,\mu\text{m}^{-1}$. For $d = 50\,\mu\text{m}$ this corresponds to amplification ratio $K_{||}/K_{\perp} \approx 1.6$. The latter determines a dynamic range of possible field controlled amplification.

3. INTEGRATED PLANAR OSCILLATOR-AMPLIFIER STRUCTURE

The sketch of this device is shown in the right-up corner of Figure 5. An oscillator CLC cell A is of standard type: it consists of two thin (0.8 mm) glasses, inner surfaces of which are treated as explained in the previous section to provide a uniform planar structure of CLC. The gap between glasses is 50 μm. The oscillator cell is filled with a dye doped cholesteric mixture. Another, narrower cell B, *attached to the first one*, is made of similar 0.8 mm thick glasses separated by 200 μm Mylar stripes. The cell B was filled with concentrated ($c = 1 \cdot 10^{-2}$ M/L or 0.5 wt.%) amplifying solution of dye Rhodamine-640 (Rh640 for brevity, from Exciton) in glycerin. The cell construction allows the independent emission measurements

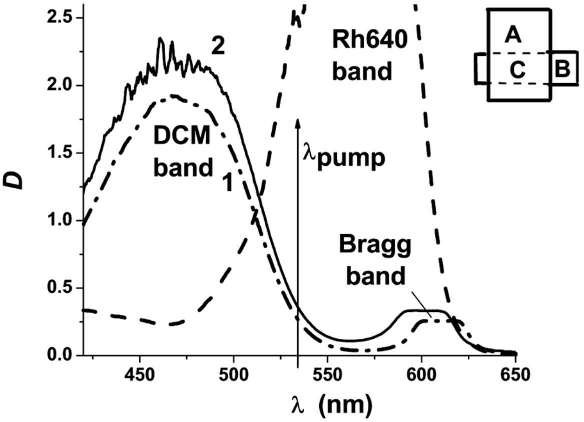

FIGURE 5 Optical density (D) spectra of 50 μm thick cells filled with CLC621 (1), CLC614 (2), which show the band of the DCM dye with $\lambda_{\max} = 467$ nm and Bragg stop band in the range of 580–630 nm. The dash-dotted line shows optical density of 200 μm thick cell filled with dye Rh640 solution in glycerin ($D_{\max} = 6.4$ at $\lambda_{\max} = 573$ nm is estimated from the measurements on a thinner cell). Two CLC generate at $\lambda \approx 621$ and 614 nm, respectively.

separately from the CLC oscillator (pump beam position A in the sketch), from the amplifier (position B) and from the sandwich formed by the two (position C).

A scheme of the measurements carried out in the Calabria University was slightly different from the described above. The device was pumped using the second harmonic of a Q-switched Nd^{3+} laser (Surelite-II by Continuum, $\lambda = 532$ nm, $\tau = 5$ ns and $f = 5$ Hz). The light beam with variable intensity was incident normally to the structure from the CLC side. It was always focused onto the amplifier cell in a spot of diameter 0.5 mm using a spherical lens of 100 mm focal length. The spectra and energy of the device emission were measured in the direction coaxial with the pump beam using an AvaSpec-2048 CCD spectrometer (resolution 0.6 nm) equipped with a collimating system.

We used the same amplifying cell that could operate with two CLC oscillators (CLC614 and CLC621) differing by the spectral positions of the Bragg band and generated emission wavelength ($\lambda_g \approx 614$ and 621 nm), Figure 5. The two mixtures are based on the nematic composition MLC-6815 (Merck) and chiral compound ZLI-811 (Merck) with different concentration of the latter (24.05% for CLC614 and 23.95% for CLC621). Tuning the mixture content was necessary to have the

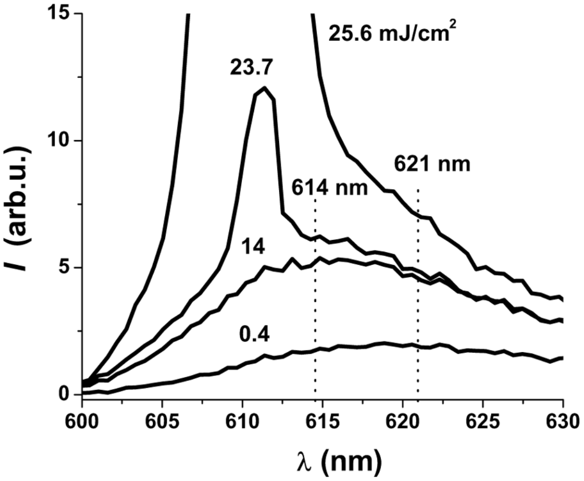

FIGURE 6 ASE intensity spectra I (λ) of Rh640 solution in glycerin at different values of pump fluence shown at the curves. Two dotted vertical lines show the position of CLC oscillator bands at 614 and 621 nm.

oscillator lasing band close to the Rhodamine-640 ASE spectrum shown in Figure 6. Both mixtures were doped with the same amount (0.6 wt.%) of laser dye DCM (4-(Dicyanomethylene)-2-methyl-6-(4-dimethyl-amino-styryl)-4*H*-pyran, Exciton). This dye absorbs only 28% of the pump beam at 532 nm, see Figure 5, therefore, our CLC oscillators work in the relatively soft conditions and the 200 μm thick Rhodamine-640 layer uses all the transmitted pump light for amplification of weak CLC emission.

In Figure 6, the ASE spectra of the pure amplifying solution is shown for variable pump fluence. These emission spectra were measured in zone B of the device. With increasing fluence we observe a shift of the luminescence maximum from 619 to 610 nm, a nonlinear growth of output energy and dramatic narrowing of the spectra, see Figure 7. Nevertheless, the positions of the amplified oscillator bands, shown in Figure 6 by dotted vertical lines, remain at the same place. Figure 8 shows a representative spectrum of non-amplified laser emission from the CLC614 oscillator at rather high pump fluence of $I_p = 45\,\mathrm{mJ/cm^2}$ (the dashed curve with 10 times blown intensity). This spectrum is somewhat broadened. After amplification by the Rh640 layer (solid curve) it becomes narrower.

Figure 9 shows how the emitted energy of CLC614 cell is amplified with increasing pump beam energy I_p. For curve CLC614, the

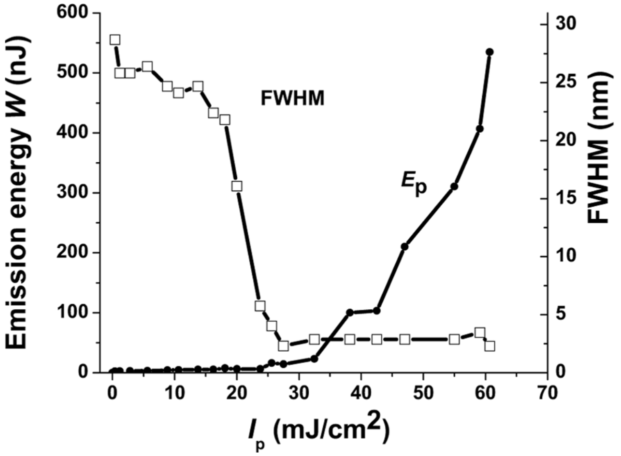

FIGURE 7 Output emission energy W and the full width at half maximum (FWHM) of the emission spectra of Rh640 amplifying cell as function of pump fluence I_p.

pump spot was located on a single CLC layer within zone A shown in the sketch in Figure 5. For curve CLC614 + Rh the pump spot is located in zone C where the CLC emission is amplified by the

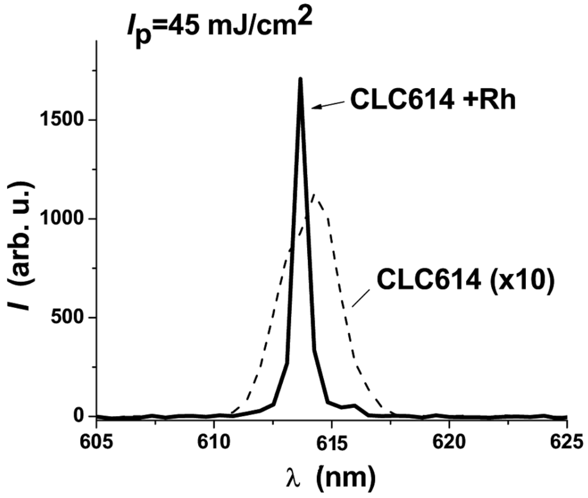

FIGURE 8 Representative spectra of non-amplified laser emission intensity I from the CLC614 oscillator (the dashed curve with 10 times blown intensity) and the same emission amplified by Rh640 layer (solid curve). Pump fluence $I_p = 45\,\text{mJ/cm}^2$.

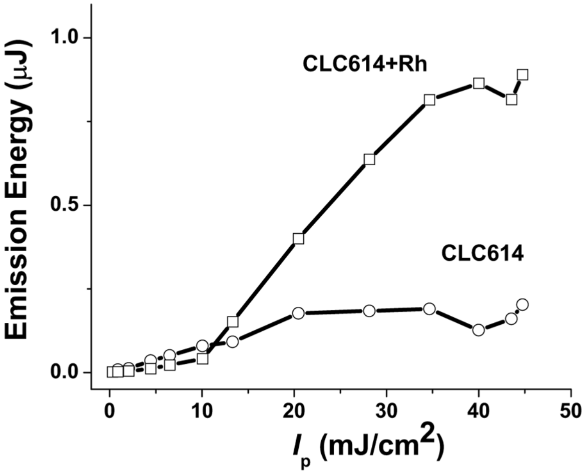

FIGURE 9 Pump fluence dependence of the energy of laser emission *W* from CLC614 cell (curve CLC614) measured in zone A of the device shown in Figure 5, and the emission energy from the same cell amplified by Rh640 solution (curve CLC + Rh) measured in zone C.

Rh640 dye. With increasing pump fluence above 10 mJ/cm^2 the CLC emission is amplified. The maximum amplification coefficient observed for CLC614 cell is $K_{\max} = 6$ at $I_p = 40\,\mathrm{mJ/cm^2}$ (for CLC621 cell $K_{\max} = 5$ at 47 mJ/cm^2). The amplification process does not change the spectral position of the oscillator bands. This is shown in Figure 10 for oscillator CLC614. The two curves for incoming (CLC614) and amplified (curve CLC614 + Rh) signals coincide with each other to accuracy of our spectrometer resolution (0.6 nm). At the same time, with increasing pump the ASE spectral maximum for Rh640 (in zone B of the device) markedly shifts from 619 to 610 nm. This is shown by curve Rh640 in Figure 10. Therefore we clearly see the locking effect of the incoming signal.

The gain index of the Rh640 cell calculated from Equation (1) and experimental data at two different wavelengths determined by two oscillators CLC614 and CLC 621 is shown in Figure 11 as a function of the pump fluence. At low I_p, instead of amplification, we observe the negative gain values due to absorption of the oscillator emission, especially pronounced for CLC614. This corresponds to the tail of the absorbance spectrum of Rh640 shown in Figure 5. The maximum gain corresponds to 96 and 81 cm^{-1} at $\lambda = 614$ and 621 nm, respectively.

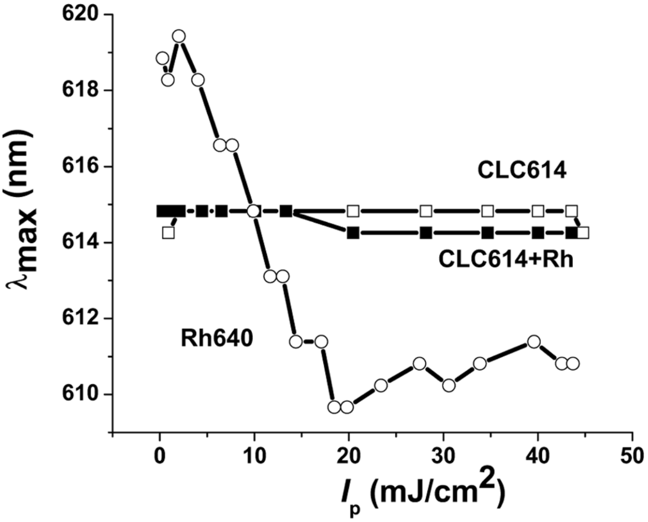

FIGURE 10 Pump fluence (I_p) dependence of the wavelength $\lambda_{\max}$ for the laser emission spectral maximum for single CLC614 oscillator (curve CLC614) and $\lambda_{\max}$ for the emission of the same cell amplified by the Rh640 cell (curve CLC614 + Rh). Curve Rh640 shows the pump fluence dependence of $\lambda_{\max}$ of the spontaneous emission of a single Rh640-glycerine cell.

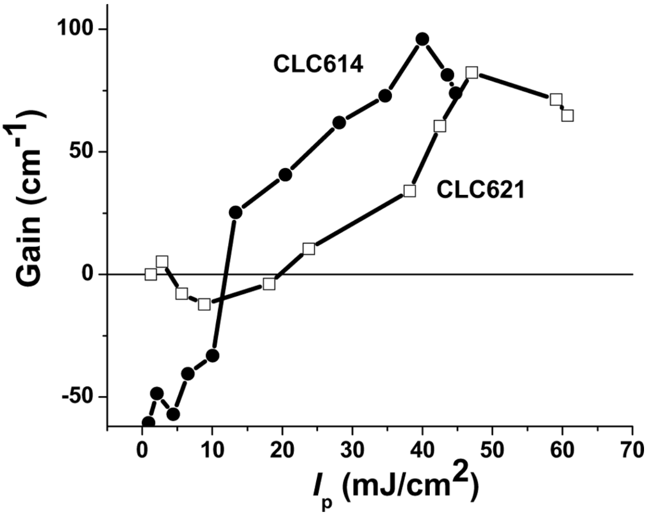

FIGURE 11 Gain index α of the amplifying cell at two different wavelengths, $\lambda = 614\,\text{nm}$ (curve CLC614) and $\lambda = 621\,\text{nm}$ (curve CLC621) as a function of pump fluence I_p.

4. DISCUSSION AND CONCLUSION

Figures 2 and 11 show that using planar amplifying structures with a gain distance as short as 50–200 μm one can obtain substantial amplification of weak emission of CLC microlasers. To this effect, the gain index must be extraordinary high. Indeed, we have obtained gain index values of about 90 cm^{-1} for the glycerin solution of Rh640 and of about 530 cm^{-1} for Chromene-3 in our nematic matrix. Probably, these are the highest values of dye gain ever reported. The reason is that we have used very dense solutions of dyes (10^{-2} M/L for Rh640 and $6 \cdot 10^{-3}$ M/L for Chromene-3) and very high pump fluence (up to 60 $\mathrm{mJ/cm^2}$ or 10 $\mathrm{MW/cm^2}$). A simple calculation of gain for different population of the upper lasing level using experimental values for absorption and emission cross-sections of the Rh640 molecule [19] has shown that, in order to obtain $\gamma \approx 100\,\mathrm{cm}^{-1}$, it is sufficient to have 12% dye molecules in the excited state. This figure seems to be reasonable. The same simple estimation for our Chromene-3 solution having $\gamma \approx 530\,\mathrm{cm}^{-1}$ results in the value of 80–90% of the total number of molecules excited to the upper laser level. However, the situation with Chromen-3 is more difficult because its luminescence spectrum dramatically changes with increasing pump fluence, see Figures 1 and 2. Evidently, an application of a simple model to the system with such a complex energy spectrum is not well justified. The large values of gain index obtained are also consistent with our calculations of the threshold gain for the CLC oscillators and the planar Fabri-Perot NLC cells having the thickness close to the experimental ones, 30–50 μm. In calculations we used the analytic approach [6] and a software based on exact solutions of the Maxwell equations [20].

It is important to understand why, at the same pump fluence, the 200 μm thick Rh640 cell has shown a smaller gain than 50 μm thick NLC cell with a Chromene-3 dye. Firstly, from Figure 5 is seen that at the pump wavelength, the optical density is about 2.5, therefore 90% of the pump light is absorbed in the frontal 80 μm layer and the remaining part is excluded from the amplification. It means that the gain index in the pumped layer is about 250 cm^{-1} or so. Secondly, in the experiment with Chromen-3, tuning of the CLC lasing spectrum to the amplifier cell luminescence spectrum is almost ideal (only 2 nm difference). However, for the Rh640 cell, due to the shift of the ASE peak of the dye with pump fluence this difference reaches 5 or even 12 nm for the two oscillators studied. Thirdly, the energy of the input beam is larger in case of the Rh614 amplifier (about 100 nJ), as compared to energy 1–2 nJ (Fig. 3) in the case of

Chromene-3/NLC cell. Consequently, the Rh614 amplifier is strongly saturated by the input signal. On the other hand the energy of the amplified beam after the Rh640 amplifier (about 1 μJ) is much larger than in the case of Chromen-3NLC amplifier (about 30 nJ). We see that each time the optimum device parameters should be selected for a particular application.

In conclusion, we have shown a possibility for amplification of weak emission intensity of microlasers based on cholesteric liquid crystals using thin planar layers of both isotropic dye solutions and dye doped nematic liquid crystals. Very high gain index values (up to 500 cm^{-1}) and absolute amplification of about 15 have been demonstrated. Especially important is the anisotropy of gain in nematics, which allows the field control of the light amplification by an electric field. The planar amplifiers on nematic liquid crystals can easily be integrated within single planar devices together with DFB microlasers based on cholesteric liquid crystals. In a particular example of such a hybrid structure, 6-times amplification of a CLC microlaser intensity and 1 μJ output signal have been achieved.

REFERENCES

[1] Lodahl, P., van Driel, A. F., Nikolaev, I. S., Irman, A., Overgaag, K., Vanmaekelbergh, D., & Vos, W. L. (2004). *Nature*, *430*, 654.

[2] Busch, K. & John, S. (1999). *Phys. Rev. Lett.*, *83*, 967.

[3] Il'chishin, I., Tikhonov, E., Tishchenko, V., & Shpak, M. (1980). *JETP Lett.*, *32*, 24.

[4] Kopp, V. I., Zhang, Z.-Q., & Genack, A. Z. (2003). *Progress in Quantum Electronics*, *27*, 369.

[5] Chanishvili, A., Chilaya, G., & Petriashvili, G. *et al.* (2005). *Appl. Phys. Lett.*, *86*, 051107.

[6] Palto, S. P. (2006). *JETP*, *103*, 472.

[7] de Gennes, P. G. (1968). *Solid State Commun.*, *6*, 163.

[8] Belyakov, V. A. & Kats, E. I. (2000). *JETP*, *91*, 488.

[9] Palto, S. P. (2002). *JETP*, *94*, 260.

[10] Palto, S. P. & Blinov, L. M. (2005). *J. Soc. Elect. Mat. Eng.*, *14*, 115.

[11] Blinov, L. M. & Chigrinov, V. G. (1993). *Electrooptic Effects in Liquid Crystal Materials*, Springer: New York.

[12] Huth, B. G. (1970). *Appl. Phys. Lett.*, *16*, 185.

[13] Hänsch, T. W., Varsanyi, F., & Schawlow, A. L. (1971). *Appl. Phys. Lett.*, *18*, 108.

[14] Basov, N. G. *et al.* (1968). Regenerative laser amplifiers. In: *Quantum Electronics in Lasers and Masers*, Skobel'tsyn, D. (Ed.), Consultants Bureau: New York, Vol. 31, 67–86.

[15] Blinov, L. M. Cipparrone, G., Mazzulla, A., Pagliusi, P., & Lazarev, V. V. (2007). *J. Appl. Phys.*, *101*, 053104-1.

[16] Blinov, L. M., Cipparrone, G., Lazarev, V. V., Pagliusi, P., Rugiero, T., & Umanskii, B. A. (2007). *J. of Nonlinear Optical Physics & Applications*, *16*, 519.

[17] Shtykov, N. M., Barnik, M. I., Blinov, L. M., Umanskii, B. A., & Palto, S. P. (2007). *Pis'ma Zh. Eksp. Teor. Fiz.*, *85*, 734.
[18] Yariv, A. (1975). *Quantum Electronics*, John Wiley & Sons, Inc.: New York.
[19] Blinov, L. M., Cipparrone, G., Lazarev, V. V., & Umanskii, B. A. (2007). *Appl. Phys. Lett.*, *91*, 061102.
[20] Palto, S. P. (2001). *JETP 92*, 552.